Local variation of inundation, sedimentary characteristics, and mineral assemblages of the 2011 Tohoku-oki tsunami on the Misawa coast, Aomori, Japan.

Yugo Nakamura [a,*]

Yuichi Nishimura [a]

Purna Sulastya Putra [b]

[a] Institute of Seismology and Volcanology, Faculty of Science, Hokkaido University, Hokkaido University, N10W8 Kita-ku Sapporo, Hokkaido 060-0810, Japan.

[b] Institute of Seismology and Volcanology, Graduate School of Science, Hokkaido University, Hokkaido University, N10W8 Kita-ku Sapporo, Hokkaido 060-0810, Japan.

* Corresponding author at: Institute of Seismology and Volcanology, Faculty of Science, Hokkaido University, N10W8 Kita-ku Sapporo, Hokkaido 060-0810, Japan. Tel.: +81-11-706-3552, fax.: +81-11-746-7404

E-mail address: nyugo@mail.sci.hokudai.ac.jp (Y. Nakamura)

Abstract

The 2011 Tohoku-oki tsunami caused severe damage to the coastal regions of eastern Japan and left a sediment veneer over affected areas. We discuss differences in depositional characteristics of the 2011 Tohoku-oki tsunami from the viewpoint of the sediment source, coastal topography and flow height. The study area on the Misawa coast, northern Tohoku, includes a 20 km long coastline with sandy beaches, coastal dunes and a gently sloping lowland. This landscape assemblage provides an opportunity to examine the effects of topography on the characteristics of the tsunami deposit. During field surveys conducted from April 10 to May 2, 2011, we described the thickness, facies, and structure of the tsunami deposit. We also collected sand samples at approximately 20 m intervals along 13 shore-perpendicular transects extending up to 550 m inland, for grain size and mineral assemblage analysis. The tsunami flow height was estimated by measuring the elevation of debris found in trees, broken tree limbs, or water marks on buildings.

The nature of the coastal lowland affected the flow height and inundation distance. In the southern part of the study area, where there is a narrow, 100 m wide low-lying coastal strip, the run-up height reached 10 m on the landward terrace slopes. To the north, the maximum inundation reached 550 m with a run-up height of 3.2 m on

the wider, low-lying coastal topography. The average flow height was 4-5 m.

The tsunami eroded coastal dunes and formed small scarps along the coast. Immediately landward of the coastal dunes the tsunami deposit was more than 20 cm thick, but thinned markedly inland from this point. Close to the dunes the deposit was composed largely of medium sand (1-2 Φ) with planar and parallel bedding, but with no apparent upward fining or coarsening. The particle size was similar to that of the coastal dune and we infer that the dunes were the local source material for the tsunami deposit at this point. The mineral assemblage of the tsunami deposit was dominated by orthopyroxene and clinopyroxene and was also similar to the dune and beach sand. At sites more than half the inundation distance inland, the thinner tsunami deposit consisted mainly of fine sand (2.375 Φ) with some upward fining. The difference in particle size and sedimentary characteristics was probably caused by differences in sediment transportation and depositional processes. We infer that the well-sorted, finer sediments were deposited out of suspension, whereas the relatively coarse sands were laid down from traction flows. The depositional characteristics of the 2011 Tohoku-oki tsunami deposit appeared to have been affected mainly by the coastal topography and the extent of erosion at any one point, as opposed to flow height.

Keywords: 2011 Tohoku-oki tsunami deposit; grain size; mineral composition; run-up height; transportation modes; topography

1. Introduction

The magnitude 9.0 earthquake on March 11, 2011, off the Pacific coast of Tohoku, Japan, was followed by a tsunami that devastated the Japan's eastern coast. The 2011 Tohoku-oki tsunami reached maximum tsunami run-up heights of 35-40 m between 38°N and 40°N, with a maximum inundation distance of 10 km inland (The 2011 Tohoku Earthquake Tsunami Joint Survey Group, 2011; Mori et al., 2012). The tsunami resulted in nearly 19,000 dead and/or missing and caused extensive and severe structural damage to much of the built environment of eastern Japan. Sandy sediments were deposited on coastal lowlands over wide areas as a result of tsunami inundation.

The distribution, composition, and sedimentary structures of several modern tsunami deposits have been studied, including the 1992 Flores (Minoura et al., 1997; Shi et al., 1995), 1993 Okushiri (Nishimura and Miyaji, 1995; Sato et al., 1995), 1994 Java (e.g. Dawson et al., 1996), 1998 Papua New Guinea (e.g. Gelfenbaum and Jaffe,

2003), 2004 Indian Ocean (e.g. Moore et al., 2006; Bahlburg and Weiss, 2007; Hori et al., 2007; Morton et al., 2008; Paris et al., 2009), 2006 Java (e.g. Moore et al., 2011) and 2009 South Pacific (e.g. Chagué-Goff et al., 2011) tsunamis.

Many studies report that the thickness and grain size of the tsunami deposit generally decrease with increasing distance from the sea. Morton et al. (2007) studied deposits of the 1998 Papua New Guinea tsunami, the 2001 Peru tsunami, and coastal storms, and concluded that the typical tsunami deposits have a mud cap, lamina sets separated by thin mud or heavy mineral laminae, rip-up clasts, and are usually normally graded. The normal grading (upward fining) of tsunami deposit has been discussed in detail (e.g. Shi et al., 1995; Gelfenbaum and Jaffe, 2003; Smith et al., 2004; Hori et al., 2007; Srinivasalu et al., 2007 ; Morton et al., 2008), and sedimentary structures have also been extensively studied (e.g. Nanayama and Shigeno, 2006;, Choowong et al., 2008; Fujiwara, 2008). Some studies have concluded that the distribution and thickness of tsunami deposits were strongly affected by the local topography of depositional areas (e.g. Nishimura and Miyaji, 1995; Minoura et al., 1997; Hori et al., 2007). Tsunami flow heights and amount of tsunami erosion also affected deposition (e.g. Gelfenbaum and Jaffe, 2003; Richmond et al., 2011). Furthermore, the composition, grain size, thickness, and sedimentary structures of

tsunami deposits vary widely with the nature of the source material (e.g. Sato et al., 1995; Goff et al., 2012). The source of many recent tsunami sediments has been variously assigned to offshore (e.g. Gelfenbaum and Jaffe, 2003; Bahlburg and Weiss, 2007; Paris et al., 2009) or nearshore (e.g. Chagué-Goff et al., 2011) zones, while few tsunami deposits are considered to be derived from inland or beach areas (e.g. Nishimura and Miyaji, 1995; Sato et al., 1995; Shi et al., 1995; Goto et al., 2011). Sediment sources and flow conditions of tsunamis are often estimated mainly based on internal structure, grain size (e.g. Shi et al., 1995; Dawson et al., 1996; Moore et al., 2007; Narayana et al., 2007; Choowong et al., 2008), microfossils (e.g. Sawai, 2002; Sawai et al., 2009; Uchida et al., 2010; Goff et al., 2011), and mineral assemblages (e.g. Szczuciński et al., 2006 Jagodziński et al., 2009). Recently, Moore et al. (2011) discussed two modes of sediment transportation (traction and suspension) identified in the 2006 western Java tsunami deposit on the basis of grain size analysis. These event layers, however, were affected by complex local topography and did not represent typical aspects of erosion and sedimentation by large tsunamis.

We conducted field surveys focusing on the distribution, facies, and sedimentary structures of the 2011 tsunami deposits, as well as on tsunami flow height and inundation distance. The Misawa coast, northern Tohoku (Fig. 1), is characterized by a

20 km long coastline with sandy beaches, coastal dunes and a gently sloping lowland. It provides an opportunity to investigate the effects of topography on tsunami sediment characteristics. The purpose of the present study is: (1) to document the general characteristics of onshore tsunami flow behavior and sedimentation in an area with a gently sloping topography, (2) to examine the effects of topography on features of tsunami deposits, and (3) to determine the sediment sources and transportation modes based on granulometric and mineral analyses.

2. Methodology

2.1. Field surveys

Field surveys were conducted from April 10 to May 2, 2011. Detailed investigations were made along 13 shore-perpendicular transects extending up to 550 m inland (Fig. 1). The elevation and distance of study points were surveyed using a total station (Nikon Total Station Nivo$^{5.SC}$). Flow height was estimated by measuring the height of broken tree limbs, debris in trees, and water marks on buildings. The inundation limit was determined by debris found piled up on the ground and the

run-up height is estimated by its elevation. We described the thickness, facies, and structures of the tsunami deposits at 140 sites, at approximately 20 m intervals along the transects. Sand samples were collected for grain size and mineral assemblage analyses at 20 sites along five transects (Transect 1, 3, 6, 7, and 10. Fig. 1), which represented a general thinning inland trend. Thirty three tsunami sand samples were taken from sites behind coastal dunes, about halfway of the inundation area, and near the inundation limit, and these tsunami deposits seemed not to be weathered or disturbed. Bulk samples of the deposit were collected, but, at locations where the thick deposit showed internal structures (e.g. laminations or significant variation of grain size and mineral composition), samples were taken from each subunit. Coastal dune sediments and beach sand were also collected along each transect.

2.2. Grain size and mineral assemblage analysis

Each sample collected from the field was washed several times by hand using tap water to remove mud and organic matter, and dried at 80 °C. The tsunami deposit in Misawa contained hardly any mud fraction. The mud contents of the relatively fine samples (A6, B, F, M4, and T) were less than 1%, except for one sample (1.7%).

Therefore the processed sample was representative of the 2011 deposit. In order to determine the grain size distribution, 10-30 g of dry sample was sieved using a set of 21 sieves with mesh sizes ranging from 0.062 mm to 2 mm (-1 Φ to 4 Φ) with 1/4 Φ intervals. Basic statistics for grain size analysis, such as mode, mean, standard deviation, skewness, and kurtosis, were calculated following the method outlined in Dawson et al. (1996). At least 200 grains in the 1.75-2.00 Φ fraction were examined under a stereo microscope for the purposes of describing the mineral assemblage.

3. Study area

The Misawa coast study area is located 320 km north-northwest of the epicenter of the 2011 Tohoku earthquake and is characterized by a virtually straight 20 km long coastline. In the southern part of the study area (around Transects 11-13), the coastal lowland is around 100-200 m wide and its landward extent is marked by a 10-15 m high terrace scarp. The coastal lowland widens up to 580 m in the northern part of the study area. There is a single coastal dune ridge parallel to the shoreline in the southern part (Fig. 2 A, B), and two or three lines of dune in the northern part of the study area. Each coastal dune is 30-100 m wide and 2-3 m high (from the base of the

dune). The dune bordering the beach is covered by herbaceous plants and shrubs, while the dunes more than 200 m inland from the coast are covered by conifer forest. These dunes are presumed to have formed in the Holocene based on the analogy of the coastal dunes 50 km north of Misawa, which formed 6,000 yrs BP or later (Chigama et al., 1998; Okamoto et al., 2000). Areas behind the coastal dunes are covered with sandy soil or dune sand as opposed to marsh or wetland. About 100 m long breakwaters perpendicular to the shoreline are located at intervals of 1 km along the coast while the area south of Transect 10 also has a series of seawalls (Figs. 1c and 2 C) along the shoreline. Coastal forests of Black Pine (*Pinus thunbergii*, Fig. 2 D) cover the area between the dunes and the main road (Route 338). These forests were destroyed by the 1896 and 1933 tsunamis, but sustained little damage from the 2011 event.

4. Flow height and flow direction of the 2011 tsunami on the Misawa coast

We measured run-up and flow heights of the 2011 Tohoku-oki tsunami along 13 shore-perpendicular transects. Fig. 1 shows the location of transects and Fig. 3A the topographic profiles from the shore to run-up limits with flow heights obtained from damaged trees. The average run-up height of the 2011 tsunami on the Misawa coast

was 5.8 m above sea level (masl). The spatial distribution of run-up heights however was distinctly different between the northern and southern sections of the study area. To the south the tsunami ran up to 7.7-10.4 m with flow heights of 6.9-8.8 masl on a terrace scarp between Transects 11-13. At the northern end of the study area however, the run-up height was only 3.5 m with a flow height of 3.2 masl on the gentle slope of Transect 1. While the run-up height may have been lower at Transect 1, the tsunami reached further inland, up to 551 m as opposed to what was observed in the southern sections of the study area.

According to an eyewitness (a 40 year-old man), three tsunami waves inundated the area around Transect 10 with the last one hitting just before dusk being the largest. He reported a sand sheet covering the lowlands following the tsunami.

The average tsunami flow direction on land (Fig. 1), estimated from damaged trees and grasses, was N74°W. These indicated an incoming flow while no evidence for return flow was noted.

5. Onshore erosion by the tsunami

On Transects 3-11, the tsunami eroded the landward face of sand dunes (Fig. 2A)

and formed up to 100 cm high scarps with channels at their base. On Transect 1, 50-100 cm of the surface were eroded across an area up to 120 m wide landward of the dunes. The tsunami also eroded along scarps on the dunes surface where paths and river channels cut across on Transects 1, 3, 4, 7, 8, 9, 10, and 11 (Fig. 2B). However, most dune top surfaces were still covered with grass, suggesting that they were not eroded or overtopped.

6. Description of depositional characteristics

6.1. Distribution and thickness of the tsunami deposit

The 2011 tsunami deposit in Misawa comprised sand grains without gravels and was underlain by a dark colored forest soil or fresh litter layer. The contrast between the tsunami deposit and the underlying soil layer was sharp and it made the identification of the deposit easy. In the forest, the 2011 deposit was not only covered with freshly fallen leaves but it also contained some that had been stripped off the trees by seawater at the time of inundation. The humic soil layer beneath the 2011 deposit was thin (less than 7 cm) and was underlain by a sandy layer of old dune.

Fig. 3B shows the thickness distribution of the 2011 tsunami deposit in Misawa and Fig. 4 shows schematic plan views along typical transects. The maximum thickness in the study area was 56 cm and was observed behind the coastal dune 87 m landward from the shore on Transect 5. Along eight of the transects (Transects 1, 2, 3, 5, 7, 8, 10, and 11) the deposit reached a maximum thickness just behind the dune and decreased rapidly inland, although thin sand sheets were still visible almost as far inland as the run-up limit as shown in Fig. 4A. The deposit thickness increased slightly in local depressions in the middle of Transects 9 and 13. Along Transects 12 and 13, where concrete seawalls (Fig.2 C) faced the shore, the deposit was relatively thin (less than 5 cm) and sometimes patchy (Fig. 4B). Although the seaward side of the dune is covered with concrete on Transect 11, the tsunami eroded the landward surface and deposited a sand layer up to 16 cm thick behind the dune.

6.2. Sedimentary structures

We observed sedimentary structures of the 2011 tsunami deposit at 140 sites on the 13 transects. The deposit appeared massive at most sites, and showed lamination and bedding only at those near the sea (Fig. 3B). These sedimentary features were

observed between 180 m and 272 m from the sea on Transect 1, 126 m and 207 m on Transect 2, 87 m and 159 m on Transect 5, 120 m and 210 m on Transect 6, 59 m and 97 m on Transect 7, 131 m and 189 m on Transect 8, 109 m and 204 m on Transect 9, 87 m and 130 m on Transect 10, and 118 m and 134 m on Transect 11. Only planar and parallel laminations were observed, except for the thick deposits 195 m from the shoreline on Transect 1, 69 m on Transect 7, and 168 m on Transect 8 that showed cross laminations. Fig. 2E shows typical laminations as observed at 180 m on Transect 1, where the pale colored sandy deposit includes several mm thin dark colored laminae comprising heavy minerals. The 2011 deposit thinned inland and contained considerably more organic debris. No apparent laminae or grading were observed at the sites more than half the inundation distance inland (Fig.2F).

7. Particle size and mineral composition of the 2011 tsunami deposit

7.1. Particle size distributions

Particle size analyses were carried out on 33 tsunami sand samples from 20 sites (Locations A-T, Fig. 3A) and 10 beach and dune sand samples along Transects 1, 3, 6, 7,

and 10. Results (Fig. 5) show that the 2011 tsunami deposit on the Misawa coast comprises sand grains from 1-3 Φ. The mean grain size of all samples from Transect 1 is around 2.5 Φ (Table 1), indicating that sediments on this transect are finer than those on the others (1.5-2.0 Φ).

Results from the five transects show that tsunami sediments generally fine inland (Fig. 5). As shown in Fig. 5 and Table 1, 18 tsunami sand samples have a mode of 2.375 Φ and seven have two different modes (1-2 Φ and 2.375 Φ). Sediments at sites more than half the inundation distance inland (Samples-C, F, G, K, L, N, O, R, S, and T) have a mode of 2.375 Φ. The only exception to this is Sample B. On Transect 1, the mean at Location A (Samples A1-A6) is 2.53-2.75 Φ: it is finer than those of beach and dune sand but coarser than the Location B sediment (2.75 Φ). A similar trend is observed on other transects with the sediments at sites more than half the inundation distance inland being 0.5-0.6 Φ finer than those from other sites near the coast. The samples from Locations C and G are coarser than other tsunami sediments, beach sand, and dune sand on each transect.

Standard deviations of most samples show little variation, ranging between 0.5-0.7 (Table 1), indicating a well to moderately sorted sand. Samples A1-A6 and the beach sand of Transect 1 are better sorted (standard deviations of 0.4-0.5). On the

other hand, samples from near the inundation limits on Transects 1, 6, and 7 are more poorly sorted. The skewness of most samples is less than zero and shows coarse-tailed distributions. The skewness of sand layers from Transect 7 though is greater than that of samples from other transects. Near the inundation limit, skewness tends to be low (Transect 6, 7, and 10), while kurtosis tends to be high (Transects 1, 3, 7, and 10) (Table 1).

7.2. Vertical variations

The 2011 deposit does not exhibit any obvious grading but the results of particle size analyses show vertical size variations. At Location A (Transect 1) and Location M (Transect 7), samples from each sub-unit (Fig. 6) were analyzed for grain size. The results from Location A (Samples A1-A6, Fig. 5) reveal that the mean grain size of the lower (Sample A6) and middle (Sample A3) parts are 2.75 Φ and 2.53 Φ, respectively (Table 1). This represents an upward coarsening in the lower two thirds of the layer. The top part (A1) is relatively finer at 2.64 Φ. On the other hand, Location M on Transect 7 shows a general upward coarsening from 1.80 Φ at the bottom to 1.56 Φ at the M3 horizon (Fig. 5, Table 1). This upward coarsening, however, is interrupted by

three separate horizons of finer material (Samples M4, M6, and M8) where mean grain sizes are between 2.06 and 2.15 Φ. The surface sample at Location M (Sample M1) has a mean grain size of 1.62 Φ indicating that there is a slight upward fining. The trend of vertical variations at Location M is therefore similar to that at Location A. Samples M1-M3 show a relatively higher skewness than that of others (Table 1), while standard deviation and kurtosis reveal little variation throughout the sequence of A1-A6 and M1-M9.

7.3. Mineral composition

Tsunami sediments on the Misawa coast contain abundant heavy minerals, ranging from 31% (Sample C) to 89% (Sample M1), as shown in Fig. 5. The heavy mineral assemblage consists mainly of orthopyroxene, clinopyroxene, and magnetite associated with minor amounts of olivine and hornblende while the light minerals are mainly plagioclase and quartz. Sand grains coarser than 1 Φ contain shell fragments, while those in the 1.75-2.00 Φ fraction common for the mineral assemblages have none.

The heavy mineral content tends to decrease inland. For example, on Transect 6,

the heavy mineral content is 76% at Location H, and 39% at Location L. Although this decreasing trend is variable on Transect 10, it ranges from 69% to 43%, whereas on Transect 3, it decreases from 58% to 36%, but increases again to 52% near the inundation limit (Location G).

8. Discussion

8.1. Tsunami flow height, run-up height, and coastal topography

As shown in Fig. 3A, tsunami flow and run-up height increased in the southern parts of the Misawa coast. The study area is 320 km north of the epicenter and therefore the differences in run-up height are presumed to be related to the local topography rather than distance from the epicenter. The flow heights at the shoreline were greater than the run-up heights on Transects 1, 5, and 6, where the topography is relatively gentle and the inundation distance is long. On the other hand, the run-up heights were notably greater on Transects 11, 12, and 13, where steep slopes are located only 200-300 m from the sea. Scatter diagrams (Fig. 7) showing the correlation between run-up height, slope gradient, and inundation distance indicate that the

run-up height and slope gradient show a strong positive correlation whereas the run-up height and distance are negatively correlated. Such positive correlation between run-up height and slope gradient was also reported by Szczuciński et al. (2006), who studied 2004 Indian Ocean Tsunami (2004 IOT) deposits in Thailand. Furthermore, a negative correlation between run-up height and inundation distance was found in the case of the 1992 Nicaragua tsunami by Higman and Bourgeois (2008). This implies that the onshore tsunami flow linearly loses its energy with distance and slope elevation. Thus, the tsunami run-up height is presumed to be strongly affected by onshore topography. The tsunami flow energy markedly decreases while the tsunami runs up the land surface, even if the topography is gentle.

8.2. Behavior of the onshore tsunami and sedimentary characteristics

The onshore tsunami flow direction is estimated to be N74°W and indicates the run-up flow. We could not find any evidence of return flow in damaged trees and grasses. A part of the thick sand layers immediately landward of the coastal dunes was possibly deposited by the return flow. However, these sand layers did not exhibit apparent depositional features of return flow as reported in previous studies (e.g.

Nanayama et al., 2000; Fujino et al., 2006; Nanayama and Shigeno, 2006; Fujiwara and Kamataki, 2007, 2008; Fujiwara 2008). This suggests that return flow was gentle in comparison with run-up and did not transport much sediment. Furthermore, the flat topography and coastal forests perhaps caused the weakening of run-up and return flow velocities. The energy of onshore tsunami flow is often reduced by forest vegetation, as reported following the 1998 Papua New Guinea tsunami (Hiraishi and Harada, 2003) or the 2004 IOT (Cochard et al., 2008; Tanaka et al., 2007).

Although eyewitness reported three tsunami waves, the sedimentary structures did not provide any apparent evidence of multiple inundations. The largest (third) wave most likely removed or disturbed the sedimentary structures formed by the first and second flows. The erosion of earlier tsunami deposits by later flow has indeed been reported by Fujino et al. (2006) and Choowong et al. (2008).

8.3. Deposit thickness and topography

As mentioned above, the 2011 deposit is thick on the landward sides of the coastal dunes and adjacent eroded areas with a marked inland thinning to only a few cm. In addition, the deposit distribution is thin and sparse along transects associated

with concrete seawalls (Transects 11-13). Thus, the thickness of the 2011 deposit in the Misawa area seems unrelated to flow height, but rather is affected by onshore topography and the extent of potential sediment sources and eroded areas. Similar relationships between sediment thickness and topography have been reported by many (e.g. Kitamura et al., 1961; Sato et al., 1995; Phipps et al., 2001, Goff et al., 2008; 2009; Paris et al., 2009).

8.4. Transportation modes

The grain size distributions of samples D, E, I, J, P, and Q are similar to that of dune sand. It implies that these sediments were not sorted by the transportation process. We therefore consider these sediments to be traction sediments. Moore et al. (2011) discussed formation of traction sediments in tsunami deposits, and pointed out that the material shows a trend of upward coarsening and predominantly thick deposition. On the Misawa coast, the sediments at Locations A and M show upward coarsening in the middle and lower part of the 2011 deposit. In addition, the deposit at Locations A, D, I, M, P, and Q is remarkably thick (Fig. 3 right). Therefore, the sediments shown by samples A3-A6, D, E, H, I, J, M3-M9, P, and Q are presumed to be

formed by traction flow. High percentages of heavy minerals in these samples (Fig. 5) also support this assumption. The thick deposits immediately landward of the dunes on Transects 1, 3, 5, 7, 8, 9, 10, and 11 (Fig. 3B) are also thought to be traction sediments. A tsunami deposit with upward coarsening was also identified in the 1992 Nicaragua tsunami deposit (Higman and Bourgeois, 2008) and interpreted to be traction flow sediment. Paris et al. (2009) also reported bed load sediment formed by the 2004 IOT in Sumatra.

On the other hand, sand grains around 2.375 Φ are included in the tsunami deposits near the run-up limit. These finer grained sediments are observed in many samples from the inundation area and we infer that they have been deposited out of suspension. Such sediment forms thin layers (less than 7 cm, Fig. 3) but is widely distributed. Suspension is a very common process of sediment transportation by tsunami flow and such suspension deposit has been often identified in tsunami-affected areas (e.g. Hindson and Andrade, 1999; Dawson and Smith, 2000; Gelfenbaum and Jaffe, 2003; Jaffe and Gelfenbaum, 2007; Morton et al., 2007; Peters at al., 2007; Jagodziński et al., 2009; Jaffe et al., 2011).

8.5. Source area of the tsunami deposit

A >20 cm thick tsunami deposit occurs only within 100 m of the coastal dunes, suggesting that the sediment source is either dune or beach sand. This assumption is supported by the observation of erosion of the dune surface along many transects.

Grain size distribution provides important evidence for estimating the tsunami sediment source area. Grain size distributions from Transects 3, 6, and 10 (Fig. 5) suggest that the tsunami deposit is classified into two categories: one comprising mainly 1-2 Φ sand grains (Samples D, E, H, I, J, P, and Q) and the other around 2.375 Φ (Samples F, K, L, R, S, and T). The former category has the same grain size as the local dune sand and therefore the deposit was most likely from this source (Transects 6 and 10). The mean grain sizes of samples F, K, L, R, S, and T are smaller than those of beach and dune sand. However, sand grains around 2.375 Φ are also included in the beach sand (Transects 3 and 6) and dune sand (Transects 3, 6, and 10), as shown in Fig. 5 and Table 1. We could infer that the fine sediment is from an offshore source. However, we consider that the differences in grain size distribution are due to sediment transportation modes, as mentioned above. The fine sediment was presumably separated from the dune material in the course of transportation and deposition, as discussed by Shi et al. (1995). In addition, the original beach sediment

before the 2011 tsunami is likely to be finer than our study samples collected after the event. Beach sediments before the 2004 IOT in Sumatra, Thailand, and India were reported to be finer than those after the event (Babu et al., 2007; Choowong et al., 2009; Paris et al., 2010). The mineral composition of the tsunami sediments is similar to that of the dune and beach sand on the Misawa coast and it supports this presumption that the tsunami sediment originated from a local source. As mentioned above, the source of many recent tsunami deposits is inferred to be from offshore materials as shown by Gelfenbaum and Jaffe (2003), Bahlburg and Weiss (2007), Paris et al. (2009), amongst others, thus the 2011 deposit on the Misawa coast is somewhat rare. However, studies of the 2011 Tohoku-oki deposit on the Sendai Plain 300 km from our study area have revealed that the tsunami deposit was mostly derived from local onshore sources (eg. Goto et al., 2011).

Relatively coarse tsunami sediment was observed at Location C on Transect 1 (Fig. 5). Transect 3 also presented coarser sediment at an inland site (Location G). These transects are across an older dune system which probably provided the coarser source material in these cases. Tsunami sediments at Location L (Transect 6) contain coarse particles greater than -1 Φ. When viewed under a microscope these consisted of artificial gravels and fragments of building material. This anthropogenic material was

most likely entrained during tsunami flow across the land and deposited along the transect. Samples from locations near the inundation limit tend to be relatively poorly sorted (Table 1, Samples C, L, and O), and have a low skewness (Samples B, C, L, O, and T) and high kurtosis (Samples B, C, G, O, and T), suggesting that these sediments contains local soil or older dune material.

8.6. Characteristics of heavy mineral composition

The tsunami deposit on the Misawa coast shows a lateral change of heavy mineral content, which generally tends to decrease inland. In particular, the magnetite content decreases inland markedly on Transects 1 and 3, as shown in Fig. 5. In addition, the thick deposit at Locations A and M contains abundant heavy minerals within the whole bed of sediment. These facts imply that a larger amount of heavy minerals is characteristic of traction sediment. On the other hand, relatively light materials are transported further inland as suspended sediments. A lateral and vertical change of heavy mineral assemblage was discussed by Jagodziński et al. (2009), who studied the 2004 IOT deposit in Thailand and reported an upward as well as a landward increase in flake-shaped micas in the tsunami deposit. They concluded

that the heavy mineral assemblage reflected tsunami flow conditions and the mode of sediment transportation and deposition. We infer this is applicable to the 2011 tsunami deposit on the Misawa coast.

The tsunami deposit on the Misawa coast contains abundant heavy minerals throughout as shown in the mineralogical composition of samples A1-A6 and M1-M9 (Fig. 5). Furthermore, magnetite content increases slightly upwards from sample M9 to M1 (Fig. 5). These heavy minerals are often represented by thin laminae (Fig. 2E). Tsunami deposits generally contain heavy minerals in the lower part of the layer (eg. Morton et al., 2007; Switzer and Jones, 2008; Jagodziński et al., 2009), although in a few cases heavy minerals are found throughout (e.g. Higman and Bourgeois, 2008; Morton et al., 2008). The presence of heavy mineral laminae is presumed to be controlled by the sediment transportation modes. Jagodziński et al. (2009) concluded that the relatively light minerals settle slowly from suspension. On the other hand, the thick 2011 deposit on the Misawa coast is attributed to sedimentation by traction flow. Therefore, the distribution of heavy minerals is different from that reported in many cases (eg. Morton et al., 2007; Switzer and Jones, 2008; Jagodziński et al., 2009).

Field observations of the deposit facies at locations A and M (Fig. 6) revealed five thin laminae with abundant fine grained heavy minerals (horizons A3, A6, M4, M6,

and M8). However, as the analysis of the heavy mineral assemblage was carried out on a coarser fraction (1.75-2.00 Φ), the fine grained heavy minerals were not taken into account, resulting in the apparent discrepancy between field observations (Fig. 6) and results of heavy mineral analysis (Fig. 5). The difference of mineral composition among grain size classes will be investigated in future work.

The 2011 tsunami deposit on the Misawa coast contains large amounts of heavy minerals (Fig. 5), compared with previous studies such as that of Jagodziński et al. (2009). This might be due to the presence of coastal sediments containing abundant heavy minerals and a geological substrate acting as a source of abundant heavy minerals from the adjacent regions, such as volcanics found in northern Tohoku (Editorial Committee of Tohoku, Part 2 of Regional Geology of Japan, 1989).

8.7. Application to paleotsunami research

In studies of paleotsunamis, the run-up height is often estimated from the elevation of the highest outcrop or excavation site where the deposit is observed (e.g. Dawson and Smith, 2000; Satake et al., 2005; Nanayama et al., 2007). However, as mentioned above, the tsunami run-up height is often affected by local topography and

is different from the inundation height near the coast. In addition, the distribution area and thickness of tsunami deposits are markedly small if the coastal region lacks dune, sandy beach, or eroded surfaces. The 2011 deposit on this stretch of the Misawa coast had preserved its original thickness and sedimentary structures at least one month after the event, but was already undergoing soil formation processes, such as weathering and leaf litter accumulation. Thin tsunami deposits from the 2011 event are therefore unlikely to be distinguishable from soil layers within a few years. Little is known about the process of weathering and preservation potential of tsunami deposits, despite pioneering works by researchers such as Szczuciński et al. (2006), Nichol and Kench (2008) and Szczuciński (2012). Therefore, the paleotsunami run-up height must be estimated after careful geological, geochemical, and paleontological examination of tsunami deposits (e.g. Goff et al., 2012).

The Pacific coast of Tohoku, Japan experienced tsunamis in AD869, AD1611 and AD1896. These tsunamis may also have affected the Misawa coast, but we were unable to find any paleotsunami layers beneath the 2011 deposit along the 13 studied transects on the Misawa coast. Paleotsunami deposits therefore appear difficult to identify on the Misawa coast, probably because of the sandy environment and local topographic characteristics.

8. Conclusions

The run-up height of the 2011 Tohoku-oki tsunami on the Misawa coast was approximately 5.8 masl. The spatial distribution of run-up heights however was distinctly different between the northern sections of the study area, with a run-up height of 7.7-10.4 masl, and southern ones with a run-up of 3.5 masl. The run-up height and slope gradient show a positive correlation whereas the run-up height and distance are negatively correlated. The tsunami run-up height is presumed to be strongly affected by onshore topography.

The tsunami eroded coastal dunes and small scarps along the Misawa coast. The tsunami deposit reached a maximum thickness immediately landward of these eroded areas and thinned rapidly inland up to the run-up limit. In areas where there were no eroded surfaces near the coast, the tsunami deposit was thin and sparse. Deposit thickness and grain size seemed unrelated to flow height. The tsunami deposit had a similar grain size and mineral composition to the coastal dune sand, thus suggesting it originated from this source. Effects of return flow on the depositional process are presumed to be minor.

The tsunami deposit comprised sand grains from 1-3 Φ and fines inland with the heavy mineral content decreasing at inland sites. At study sites behind the coastal dunes the sediment was more than 10 cm thick, comprised relatively coarse grains, and showed planar and parallel laminae. The lower and middle part of the sediment showed upward coarsening as shown at Location A (Transect 1) and Location M (Transect 7). This sediment is thus presumed to have been deposited out of traction flow. On the other hand, at sites more than half the inundation distance inland the sediment was thinner (less than seven cm) and comprised mainly fine sand grains, suggesting it was deposited out of suspension.

Our future work will include a detailed investigation of the tsunami deposit source and transportation mode, based on microfossil analyses such as foraminifera, ostracoda, and diatoms. Furthermore, the differences between depositional characteristics along the Misawa coast and other affected areas and those between the 2011 tsunami and paleotsunamis will be discussed based on further field work and analysis.

Acknowledgements

We thank Kei Ioki for her help with the field surveys. We also thank Dr.

Catherine Chagué-Goff for reading the manuscript and providing valuable comments, and two reviewers, Dr. James Goff and Dr. Raphaël Paris, for many constructive suggestions.

References

Babu, N., Babu, D., Das, P., 2007. Impact of tsunami on texture and mineralogy of a major placer deposit in southwest coast of India. Environmental Geology 52, 71-80.

Bahlburg, H., Weiss, R., 2007. Sedimentology of the December 26, 2004, Sumatra tsunami deposits in eastern India (Tamil Nadu) and Kenya. International Journal of Earth Sciences 96, 1195-1209.

Chagué-Goff, C., Schneider, J.-L., Goff, J.R., Dominey-Howes, D., Strotz, L., 2011. Expanding the proxy toolkit to help identify past events: Lessons from the 2004 Indian Ocean Tsunami and the 2009 South Pacific Tsunami. Earth-Science Reviews 107, 107-122.

Chigama, A., Tada S., Aonuma T., 1998. Investigation on legends in tsunamis in

Shimokita Peninsula and the formation of sand deposit to bury Hiba wood. Zisin (Journal of the Seismological Society of Japan. 2nd ser.) 51, 61-73. (in Japanese with English abstract)

Cochard, R., Ranamukhaarachchi, S.L., Shivakoti, G.P., Shipin, O.V., Edwards, P.J., Seeland, K.T., 2008. The 2004 tsunami in Aceh and Southern Thailand: A review on coastal ecosystems, wave hazards and vulnerability. Perspectives in Plant Ecology, Evolution and Systematics. Perspectives in Plant Ecology, Evolution and Systematics 10, 3-40.

Choowong, M., Murakoshi, N., Hisada, K., Charusiri, P., Charoentitirat, T., Chutakositkanon, V., Jankaew, K., Kanjanapayont, P., Phantuwongraj, S., 2008. 2004 Indian Ocean tsunami inflow and outflow at Phuket, Thailand. Marine Geology 248, 179-192.

Choowong, M., Phantuwongraj, S., Charoentitirat, T., Chutakositkano, B., Yumuang, S., Charusiri, P., 2009. Beach recovery after 2004 Indian Ocean tsunami from Phang-nga, Thailand. Geomorphology 104, 134-142.

Dawson, A.G., Shi, S., Dawson, S., Takahashi, T., Shuto, N., 1996. Coastal sedimentation associated with the June 2nd and 3rd, 1994 tsunami in Rajegwesi, Java. Quaternary Science Reviews 15, 901-912.

Dawson, S., Smith, D.E., 2000. The sedimentology of Middle Holocene tsunami facies in northern Sutherland, Scotland, UK. Marine Geology 170, 69-79.

Editorial Committee of Tohoku, Part 2 of Regional Geology of Japan, 1989. Regional Geology of Japan Part 2 Tohoku, Kyoritsu Shuppan, Tokyo, Japan (in Japanese)

Fujino, S., Masuda, F., Tagomori, S., Matsumoto, D., 2006. Structure and depositional processes of a gravelly tsunami deposit in a shallow marine setting: Lower Cretaceous Miyako Group, Japan. Sedimentary Geology 187, 127-138.

Fujiwara, O., 2008. Bedforms and sedimentary structures characterizing tsunami deposits. In: Shiki, T., Tsuji, Y., Yamazaki, T., Minoura, K. (Eds.), Tsunamiites—Features and Implications. Elsevier, pp.51-62.

Fujiwara, O, Kamataki, T., 2007. Identification of tsunami deposits considering the tsunami waveform: An example of subaqueous tsunami deposits in Holocene shallow bay on southern Boso Peninsula, Central Japan. Sedimentary Geology 200, 295-313.

Fujiwara, O., Kamataki, T., 2008. Tsunami depositional processes reflecting the waveform in a small bay: Interpretation from the grain size distribution and sedimentary structures. In: Shiki, T., Tsuji, Y., Yamazaki, T., Minoura, K. (Eds.), Tsunamiites−Features and Implications. Elsevier, pp.133-152.

Gelfenbaum, G., Jaffe, B.E., 2003. Erosion and sedimentation from the 17 July, 1998 Papua New Guinea tsunami. Pure and Applied Geophysics 160, 1969-1999.

Goff, J., McFadgen, B.G., Wells, A., Hicks, M., 2008. Seismic signals in coastal dune systems. Earth-Science Reviews 89, 73-77.

Goff, J., Lane, E.M., Arnold, J., 2009. The tsunami geomorphology of coastal dunes. Natural Hazards and Earth System Sciences 9, 847-854.

Goff, J., Lamarche, G., Pelletier, B., Chagué-Goff, C., Strotz L., 2011. Palaeotsunami precursors to the 2009 South Pacific tsunami in the Wallis and Futuna archipelago. *Earth-Science Reviews*, 107, 91-106.

Goff, J., Chagué-Goff, C., Nichol, S.L., Jaffe, B., Dominey-Howes, D., 2012. Progress in palaeotsunami research. Sedimentary Geology 243-244, 70-88.

Goto, K., Chagué-Goff, C., Fujino, S., Goff, J., Jaffe, B., Nishimura, Y., Richmond, B., Suguwara, D., Szczuciński, W., Tappin, D.R., Witter, R., Yulianto, E., 2011. New insights into tsunami risk from the 2011 Tohoku-oki event. Marine Geology, 290, 46-50.

Higman, B., Bourgeois, J., 2008. Deposits of the 1992 Nicaragua tsunami. In: Shiki, T., Tsuji, Y., Yamazaki, T., Minoura, K. (Eds.), Tsunamiites—Features and Implications. Elsevier, pp.81-103.

Hindson, R.A., Andrade, C., 1999. Sedimentation and hydrodynamic processes associated with the tsunami generated by the 1755 Lisbon earthquake. Quaternary International 56, 27-38.

Hiraishi, T., Harada, K., 2003. Greenbelt tsunami prevention in South-Pacific region. Report of the Port and Airport Research Institute 42-2, 1-23.

Hori, K., Kuzumoto, R., Hirouchi, D., Umitsu, M., Janjirawuttikul, N., Patanakanog, B., 2007. Horizontal and vertical variation of 2004 Indian tsunami deposits: An example of two transects along the western coast of Thailand. Marine Geology 239, 163-172.

Jaffe, B.E., Gelfenbaum, G., 2007. A simple model for calculating tsunami flow speed from tsunami deposits. Sedimentary Geology 200, 347-361.

Jaffe, B., Buckley, M., Richmond, B., Strotz, L., Etienne, S., Clark, K., Watt, S., Gelfenbaum, G., Goff, J., 2011. Flow speed estimated by inverse modeling of sandy sediment deposited by the 29 September 2009 tsunami near Satitoa, east Upolu, Samoa. Earth-Science Reviews 107, 23-37.

Jagodziński, R., Sternal, B., Szczuciński, W., Lorenc, S., 2009. Heavy minerals in 2004 tsunami deposits on Kho Khao Island, Thailand. Polish Journal of Environmental Studies 18, 103-110.

Kitamura, N., Kotaka, T., Kataoka, J., 1961. Coastal region between Ofunato and Shizugawa, Geological observations of the Sanriku coastal region damaged by tsunami due to the Chile earthquake in 1960. Contributions from the Institute of Geology and Paleontology of Tohoku University 52, 28-40. (in Japanese)

Minoura, K., Imamura, F., Takahashi, T., Shuto, N., 1997. Sequence of sedimentation processes caused by the 1992 Flores tsunami. Geology 25, 523-526.

Moore, A., Nishimura, Y., Gelfenbaum, G., Kamataki, T., Triyono, R., 2006. Sedimentary deposits of the 26 December 2004 tsunami on the northwest coast of Aceh, Indonesia. Earth Planets Space 58, 253-258.

Moore, A., McAdoo, B. G., Ruffman, A., 2007. Landward fining from multiple sources in a sand sheet deposited by the 1929 Grand Banks tsunami, Newfoundland. Sedimentary Geology 200, 336-346.

Moore, A., Goff, J., McAdoo, B.G., Fritz, H.M., Gusman, A., Kalligeris, N., Kalsum, K., Susanto, A., Suteja, D., Synolakis, C.E., 2011. Sedimentary Deposits from the 17 July 2006 Western Java Tsunami, Indonesia: Use of Grain Size Analyses to Assess Tsunami Flow Depth, Speed, and Traction Carpet Characteristics. Pure and Applied Geophysics DOI 10.1007/s00024-011-0280-8.

Mori, N., Takahashi, T., The 2011 Tohoku earthquake tsunami joint survey group, 2012.

Nationwide post event survey and analysis of the 2011 Tohoku earthquake tsunami. Coastal Engineering Journal 54, DOI: 10.1142/S0578563412500015.

Morton. R.A., Gelfenbaum, G., Jaffe, B.E., 2007. Physical criteria for distinguishing sandy tsunami and storm deposits using modern examples. Sedimentary Geology 200, 184-207.

Morton, R.A., Goff, J.R., Nichol, S.L., 2008. Hydrodynamic implications of textural trends in sand deposits of the 2004 tsunami in Sri Lanka. Sedimentary Geology 207, 56-64.

Nanayama, F., Shigeno, K., 2006. Inflow and outflow facies from the 1993 tsunami in southwest Hokkaido. Sedimentary Geology 187, 139-158.

Nanayama, F., Shigeno, K., Satake, K., Shimokawa, K., Koitabashi, S., Miyasaka, S., Ishii, M., 2000. Sedimentary differences between the 1993 Hokkaido-nansei-oki tsunami and the 1959 Miyakojima typhoon at Taisei, southwestern Hokkaido, northern Japan. Sedimentary Geology 135, 255-264.

Nanayama, F., Furukawa, R., Shigeno, K., Makino, A., Soeda, Y., Igarashi, Y., 2007. Nine unusually large tsunami deposits from the past 4000 years at Kiritappu marsh along the southern Kuril Trench. Sedimentary Geology 200, 275-294.

Narayana, A.C., Tatavarti, R., Shinu, N., Subeer, A., 2007. Tsunami of December 26,

2004 on the southwest coast of India: Post-tsunami geomorphic and sediment characteristics. Marine Geology 242, 155-168.

Nichol, S.L., Kench, P.S., 2008. Sedimentology and preservation potential of carbonate sand sheets deposited by the December 2004 Indian Ocean tsunami: South Baa Atoll, Maldives. Sedimentology 55, 1173-1187.

Nishimura, Y., Miyaji, N., 1995. Tsunami deposits from the 1993 southwest Hokkaido earthquake and the 1640 Hokkaido Komagatake eruption, northern Japan. Pure and Applied Geophysics 144, 719-733.

Okamoto, T., Daimaru, H., Ikeda, S., Yoshinaga, S., 2000. Human Impact on the Formation of the Buried Forests of *Thujopsis dolabrata* var. *hondai* in the Northeastern Part of Shimokita Peninsula, Northeastern Japan. The Quaternary Research (Daiyonki-Kenkyu) 39, 215-226. (in Japanese with English abstract)

Paris, R., Wassmer, P., Sartohadi, J., Lavigne, F., Barthomeuf, B., Desgages, E., Grancher, D., Baumert, P., Vautier, F., Brunstein, D., Gomez, C., 2009. Tsunamis as geomorphic crises: Lessons from the December 26, 2004 tsunami in Lhok Nga, West Banda Aceh (Sumatra, Indonesia). Geomorphology 104, 59-72.

Paris, R., Fournier, J., Poizot, E., Etienne, S., Mortin, J., Lavigne, F., Wassmer, P., 2010. Boulder and fine sediment transport and deposition by the 2004 tsunami in Lhok

Nga (western Banda Aceh, Sumatra, Indonesia): a coupled offshore-onshore model. Marine Geology 268, 43-54.

Peters, R., Jaffe, B., Gelfenbaum, G., 2007. Distribution and sedimentary characteristics of tsunami deposits along the Cascadia margin of western North America. Sedimentary Geology 200, 372-386.

Phipps, J., Jol, H.M., Peterson, C.D., Vanderburgh, S., 2001. Sand dune reactivation and subduction zone earthquakes in the Grayland area. Washington Geology 28, 31-33.

Richmond, B., Buckley, M., Etienne, S., Chagué-Goff, C., Clark, K., Goff, J., Dominey-Howes, D., Strotz, L., 2011. Deposits, flow characteristics, and landscape change resulting from the September 2009 South Pacific tsunami in the Samoan islands. Earth-Science Reviews 107, 38-51

Satake, K., Nanayama, F., Yamaki, S., Tanioka, Y., Hirata, K., 2005. Variability among tsunami sources in the 17th-21st centuries along the southern Kuril trench. In: Satake, K. (ed.) Tsunamis: Case Studies and Recent Developments. Springer, pp.157-170.

Sato, H., Shimamoto, T., Tsutsumi, A., Kawamoto, E., 1995. Onshore tsunami deposits caused by the 1993 southwest Hokkaido and 1983 Japan Sea earthquakes. Pure

and Applied Geophysics 144, 693-717.

Sawai, Y., 2002. Evidence for 17th century tsunamis generated on the Kuril-Kamchatka subduction zone, Lake Tokotan, Hokkaido, Japan. Journal of Asian Earth Science, 20, 903-911.

Sawai, Y., Jankaew, K., Martin, M.E., Prendergast, A., Choowong, M., Charoentitirat, T., 2009. Diatom assemblages in tsunami deposits associated with the 2004 Indian Ocean tsunami at Phra Thong Island, Thailand. Marine Micropaleontology 73, 70-79.

Shi, S.Z., Dawson, A.G., Smith, D.E., 1995. Coastal sedimentation associated with the December 12th, 1992 tsunami in Flores, Indonesia. Pure and Applied Geophysics 144, 525-536.

Smith, D.E., Shi, S., Cullingford, R.A., Dawson, A.G., Dawson, S., Firth, C.R., Foster, I.D.L., Fretwell, P.T., Haggart, B.A., Holloway, L.K., Long, D., 2004. The Holocene Storegga Slide tsunami in the United Kingdom. Quaternary Science Reviews 23, 2291-2321.

Srinivasalu, S., Thangadurai, N., Switzer, A.D., Ram Mohan, V., Ayyamperumal, T., 2007. Erosion and sedimentation in Kalpakkam (N Tamil Nadu, India) from the 26th December 2004 tsunami. Marine Geology 240, 65-75.

Switzer, A.D., Jones, B.G., 2008. Large-scale washover sedimentation in a freshwater lagoon from the southeast Australian coast: sea-level change, tsunami or exceptionally large storm? The Holocene 18, 787-803.

Szczuciński, W., 2012. The post-depositional changes of the onshore 2004 tsunami deposits on the Andaman Sea coast of Thailand. Natural Hazards 60, 115-133.

Szczuciński, W., Chaimanee, N., Niedzielski, P., Rachlewicz, G., Saisuttichai, D., Tepsuwan, T., Lorenc, S., Siepak, J., 2006. Environmental and geological impacts of the 26 December 2004 tsunami in coastal zone of Thailand — overview of short and long-term effects. Polish Journal of Environmental Studies 15, 793-810.

Tanaka, N., Sasaki, Y., Mowjood, M.I.M., Jinadasa, K.B.S.N., Homchuen S., 2007. Coastal vegetation structures and their functions in tsunami protection: experience of the recent Indian Ocean tsunami. Landscape and Ecological Engineering 3, 33-45.

The 2011 Tohoku Earthquake Tsunami Joint Survey Group, 2011. Nationwide Field Survey of the 2011 Off the Pacific Coast of Tohoku Earthquake Tsunami. Journal of Japan Society of Civil Engineers Series B 67, 63-66.

Uchida, J., Fujiwara, O., Hasegawa, S., Kamataki T., 2010. Sources and depositional processes of tsunami deposits: Analysis using foraminiferal tests and

hydrodynamic verification. Island Arc 19, 427-442.

Captions

Fig. 1. Location of study area and transects: (A) Japan coast and epicenter of the March 11, 2011 magnitude 9.0 earthquake, (B) Study area, (C) Transects and land use of study area (Transects extend from shoreline to tsunami run-up limit. Tsunami flow direction was estimated from damaged trees and flattened grass).

Fig. 2. Photographs showing different landscapes of the Misawa coast and features of the 2011 Tohoku-oki tsunami deposit. (A) Erosion on the coastal dune (Transect 5), (B) Erosion of the coastal dune (Transect 10), (C) The concrete seawall (Transect 12), (D) Coastal forests of Black Pine (*Pinus thunbergii*, Transect 6), (E) The 2011 tsunami deposit showing typical laminations 180 m from the sea (Transect 1), (F) Thin tsunami deposit 270 m from the sea (Loc. J, Transect 6)

Fig. 3. (A) Land surface profile, run-up height (masl), and flow height (masl) on 13 transects, (B) thickness of the 2011 tsunami deposit along the transects. Locations A-T are sediment sample sites.

Fig. 4. Schematic plan views showing distribution of the 2011 tsunami sand sheets, inundation limits, and geographic features along, (A) Transect 10 and (B) Transects 12 and 13.

Fig. 5. Grain size distribution (Φ), mineralogical composition, and heavy mineral assemblage (the latter in the 1.75-2.00 Φ fraction) of the 2011 tsunami deposits, beach and dune sand.

Fig. 6. Stratigraphy of the 2011 tsunami deposit at Location A (Transect 1) and Location M (Transect 7). Six samples (A1 – A6) were taken from Location A, and nine (M1 – M9) from Location M. Locations of the two sites are shown in Fig. 3 A. Five horizons described as "sand grains with heavy minerals" (A3, A6, M4, M6, and M8) are not shown as dominated by heavy minerals in Fig. 5, because the heavy mineral grains in these units are finer than the 1.75-2.00 Φ fraction, which has been used for heavy mineral analysis.

Fig. 7. Scatter diagrams showing (A) the correlation between run-up height and run-up distance, and (B) the correlation between run-up height and slope gradient. The slope

gradient is expressed as a ratio of the vertical interval to its horizontal equivalent along the transects. Numbers beside dots show the transect numbers.

Table 1. Basic statistics (in Φ) for grain size of the 2001 Tohoku-oki tsunami sediment on the Misawa coast. Basic statistics (mode, mean, standard deviation, skewness, and kurtosis) were calculated following the method outlined in Dawson et al. (1996).

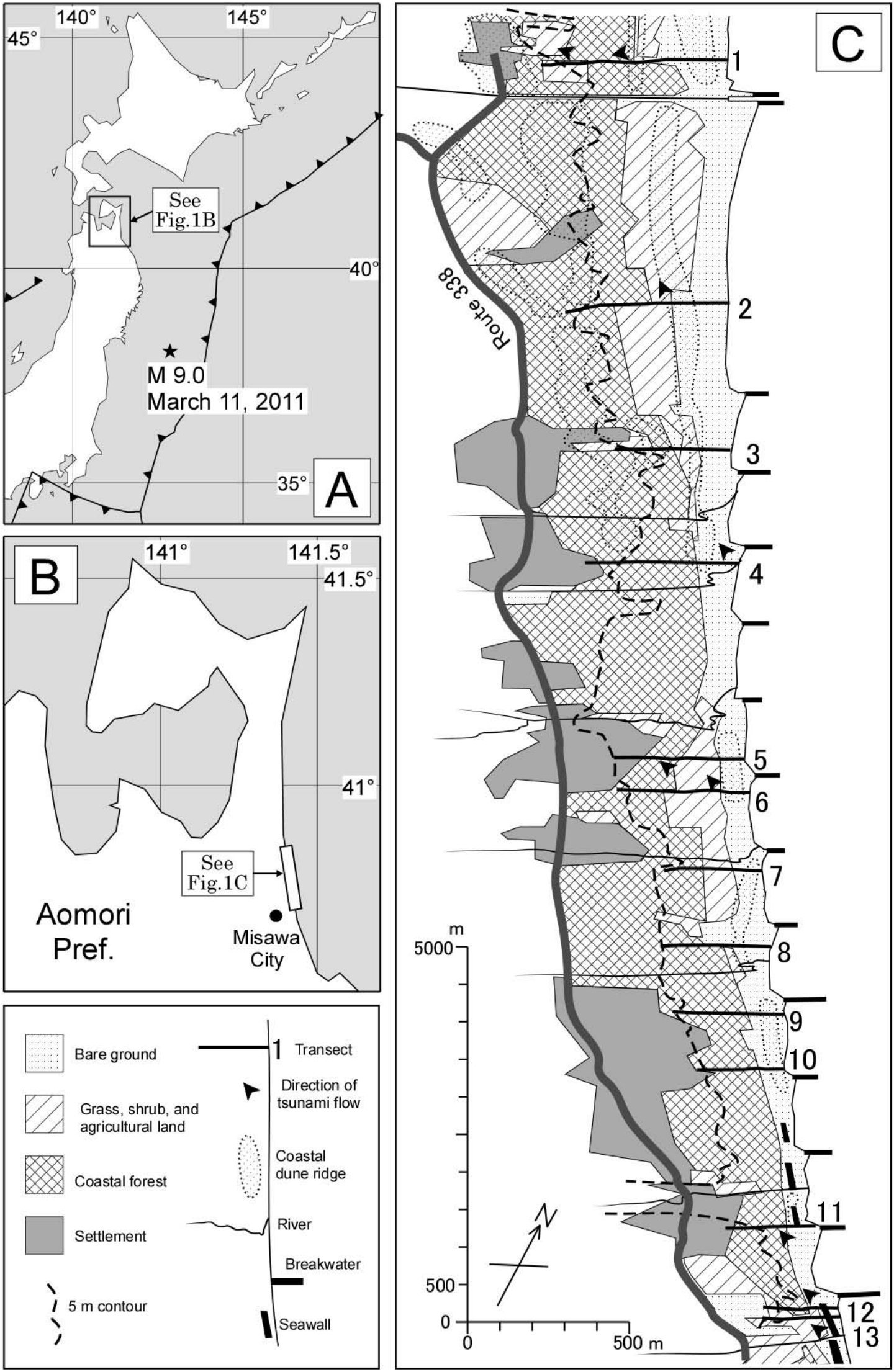
140°
145°
45°
See Fig.1B
40°
M 9.0
March 11, 2011
35°
A
B
141°
141.5°
41.5°
41°
See Fig.1C
Aomori Pref.
Misawa City
C
Route 338
1
2
3
4
5
6
7
8
9
10
11
12
13
m
5000
500
0
0
500 m
N
Bare ground
Grass, shrub, and agricultural land
Coastal forest
Settlement
5 m contour
Transect
Direction of tsunami flow
Coastal dune ridge
River
Breakwater
Seawall


A


B


C


D


E


F

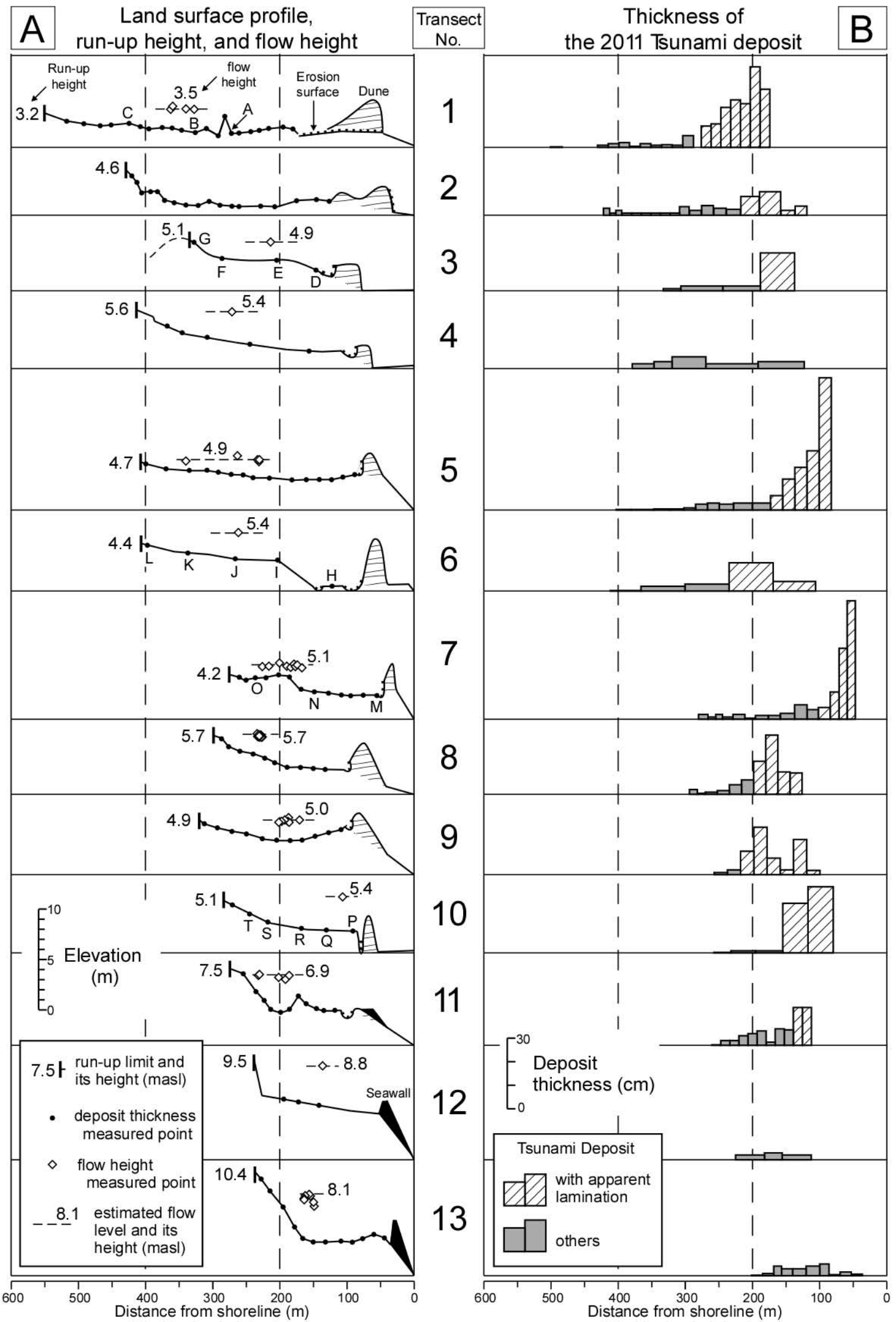
A
Land surface profile, run-up height, and flow height
Transect No.
Thickness of the 2011 Tsunami deposit
B
Run-up height
flow height
Erosion surface
Dune
3.2
3.5
C
B
A
1
4.6
2
5.1
G
4.9
F
E
D
3
5.6
5.4
4
4.7
4.9
5
4.4
5.4
L
K
J
I
H
6
4.2
5.1
O
N
M
7
5.7
5.7
8
4.9
5.0
9
5.1
5.4
T
S
R
Q
P
10
7.5
6.9
11
9.5
8.8
Seawall
12
10.4
8.1
13
10
5
0
Elevation (m)
7.5 run-up limit and its height (masl)
deposit thickness measured point
flow height measured point
8.1 estimated flow level and its height (masl)
30
0
Deposit thickness (cm)
Tsunami Deposit
with apparent lamination
others
600
500
400
300
200
100
0
Distance from shoreline (m)

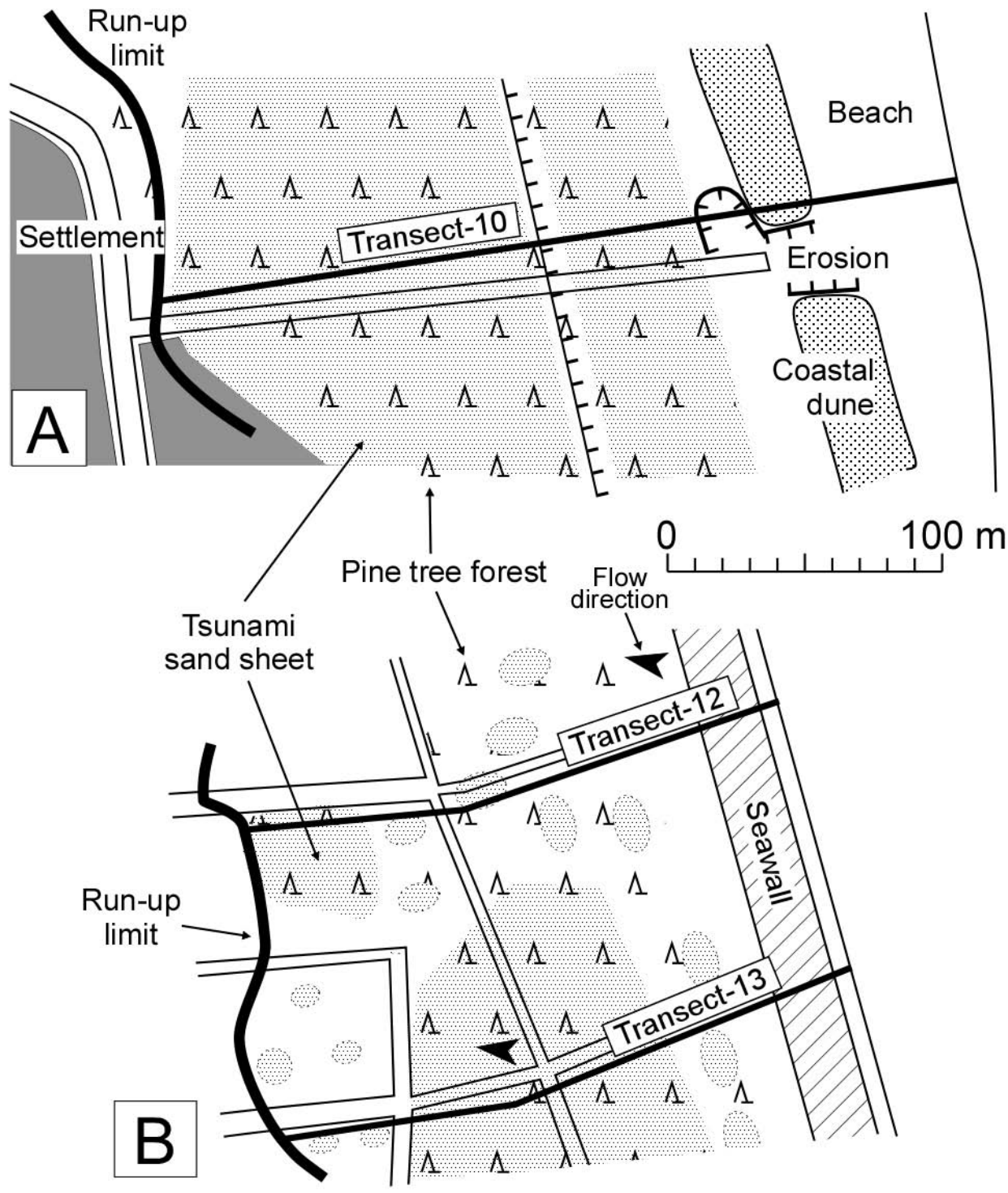
Run-up limit
Settlement
Transect-10
Beach
Erosion
Coastal dune
A
0
100 m
Pine tree forest
Flow direction
Tsunami sand sheet
Transect-12
Seawall
Run-up limit
Transect-13
B

Transect-1

Beach
Dune
A1
A2
A3
A4
A5
A6
B
C

Transect-3

Beach
Dune
D
E
F
G

Transect-6

Beach
Dune
H
I
J
K
L

Transect-7

Beach
Dune
M1
M2
M3
M4
M5
M6
M7
M8
M9
N
O

Transect-10

Beach
Dune
P
Q
R
S
T

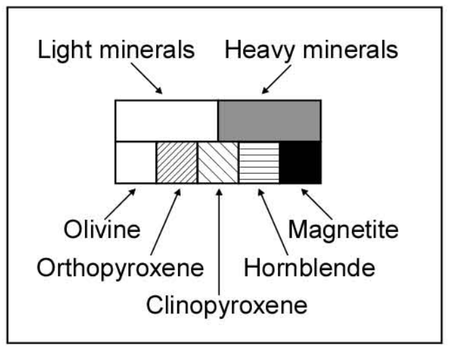

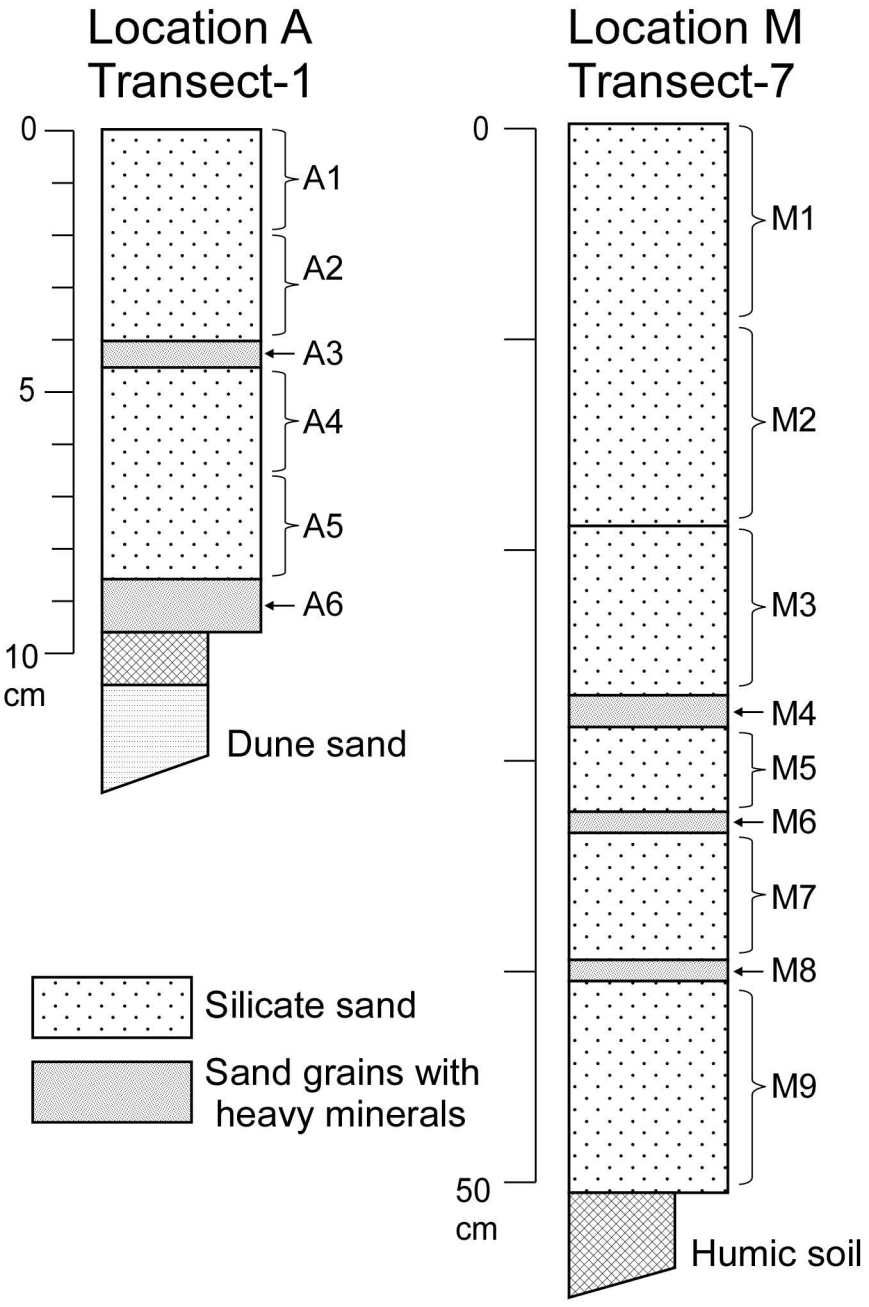
Location A
Transect-1
0
5
10
cm
A1
A2
A3
A4
A5
A6
Dune sand
Silicate sand
Sand grains with
heavy minerals
Location M
Transect-7
0
50
cm
M1
M2
M3
M4
M5
M6
M7
M8
M9
Humic soil

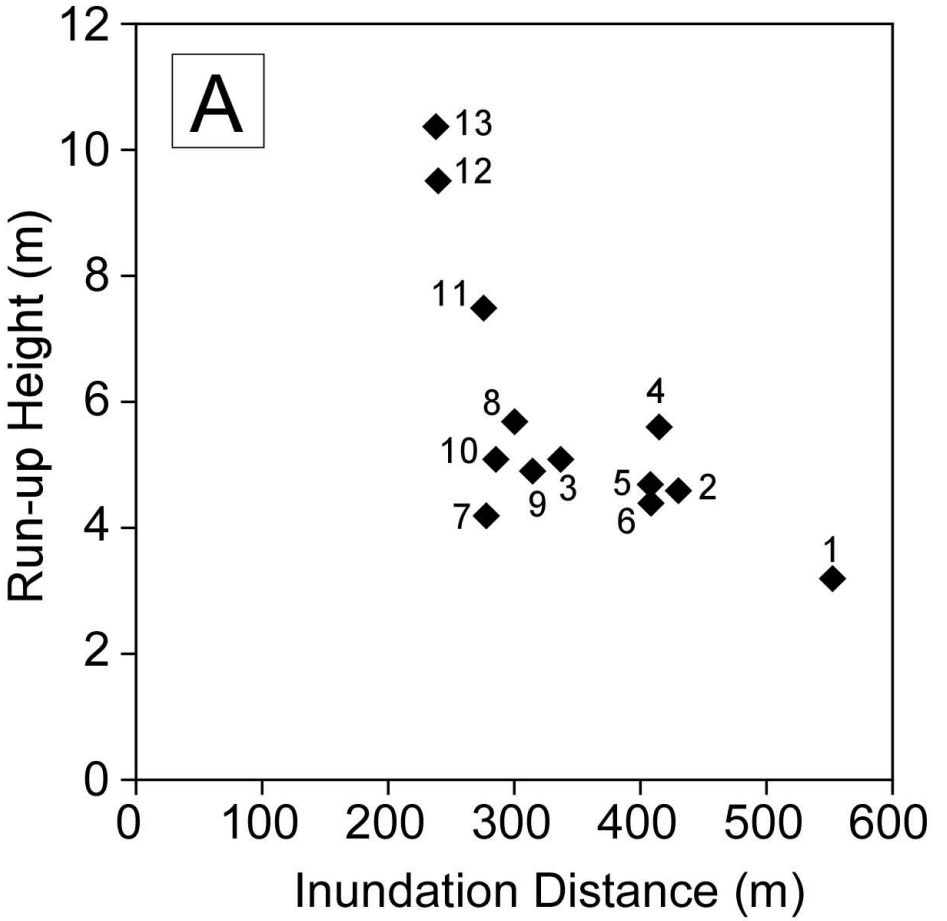
A
Run-up Height (m)
Inundation Distance (m)
0
2
4
6
8
10
12
0
100
200
300
400
500
600
13
12
11
8
4
10
3
9
5
2
7
6
1

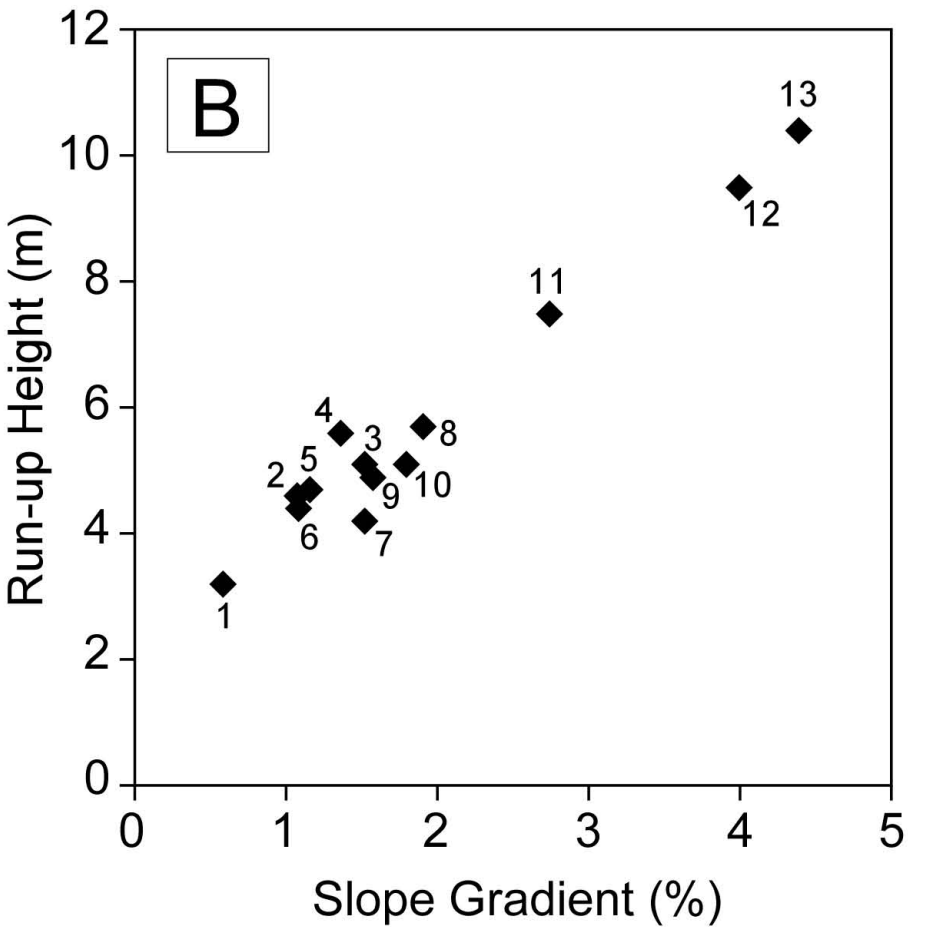
B
Run-up Height (m)
Slope Gradient (%)
0
2
4
6
8
10
12
0
1
2
3
4
5
13
12
11
4
3
8
2
5
10
9
6
7
1

Transect	Sample	mode	mean	standard deviation	skewness	kurtosis
1	Beach	2.375	2.40	0.41	-0.07	2.77
	Dune	2.375	2.23	0.60	-0.22	2.89
	A1 (0 - 2 cm)	2.375	2.64	0.45	-0.36	3.27
	A2 (2 - 4 cm)	2.375	2.55	0.47	-0.28	3.03
	A3 (4 - 4.5 cm)	2.375	2.53	0.48	-0.32	3.11
	A4 (4.5 - 6.5 cm)	2.375	2.57	0.46	-0.28	3.08
	A5 (6.5 - 8.5 cm)	2.625	2.71	0.43	-0.38	3.63
	A6 (8.5 - 9.5 cm)	2.875	2.75	0.40	-0.34	3.64
	B	2.875	2.75	0.47	-0.98	5.59
	C	2.375, 1.875	2.01	0.73	-0.71	4.75
3	Beach	2.375, 1.875	1.93	0.62	-0.66	4.10
	Dune	2.375, 1.875	1.90	0.67	-0.23	2.88
	D	2.375, 1.875	1.95	0.68	-0.18	2.78
	E	2.375, 1.875	2.17	0.63	-0.20	2.71
	F	2.375	2.57	0.53	-0.47	3.45
	G	1.375, 2.375	1.85	0.63	-0.18	3.84
6	Beach	1.375, 0.875	1.18	0.86	-0.01	2.56
	Dune	1.375, 0.875	1.52	0.74	0.34	2.80
	H	2.375, 1.875	1.96	0.58	-0.03	2.96
	I	1.375, 2.375	1.63	0.70	-0.44	4.22
	J	1.625, 2.375	1.88	0.67	-0.28	3.77
	K	2.375, 1.875	2.13	0.66	-0.36	3.50
	L*	2.375	2.24	1.15	-0.93	3.49
7	Beach	1.625	1.68	0.50	-0.09	3.86
	Dune	1.375, 2.375	1.77	0.61	0.18	2.90
	M1 (0 - 10 cm)	1.375	1.62	0.60	0.09	3.28
	M2 (10 - 19 cm)	1.375	1.60	0.62	0.04	3.00
	M3 (19 - 27 cm)	1.375	1.56	0.62	0.04	2.92
	M4 (27 - 28.5 cm)	2.375, 1.875	2.10	0.59	-0.40	3.79
	M5 (28.5 - 33 cm)	1.375, 2.375	1.63	0.68	-0.08	3.02
	M6 (33 - 34 cm)	1.875, 2.375	2.06	0.63	-0.15	3.10
	M7 (34 - 39.5 cm)	1.375, 2.375	1.80	0.65	-0.05	3.25
	M8 (39.5 - 40.5 cm)	2.375, 1.875	2.15	0.59	-0.08	2.91
	M9 (40.5 - 50.5 cm)	1.375, 2.375	1.80	0.64	-0.08	3.44
	N	2.375, 1.875	2.16	0.55	0.02	2.81
	O	2.375, 1.875	2.08	0.79	-1.16	5.91
10	Beach	0.875, 1.375	0.95	0.68	0.27	3.43
	Dune	1.875, 2.375	1.88	0.56	-0.06	3.15
	P	1.875	1.87	0.61	-0.15	3.15
	Q	1.875	1.84	0.64	-0.27	3.50
	R	2.375	2.29	0.60	-0.24	2.95
	S	2.375	2.22	0.65	-0.26	2.82
	T	2.375	2.38	0.62	-0.52	3.40

* Statistics without coarse (>-1.0 phi) grains.
Sample depths (cm) for A1 - A6 and M1 - M9 are shown with sample names.